

**MEASUREMENT OF NITRIC OXIDE PRODUCTION FROM LYMPHATIC
ENDOTHELIAL CELLS UNDER MECHANICAL STIMULI**

A Thesis

by

MOHAMMAD JAFARNEJAD

Submitted to the Office of Graduate Studies of
Texas A&M University
in partial fulfillment of the requirements for the degree of

MASTER OF SCIENCE

Approved by:

Chair of Committee,	James E. Moore, Jr.
Committee Members,	Roland R. Kaunas
	David C. Zawieja
Head of Department,	Gerard L. Cote

December 2012

Major Subject: Biomedical Engineering

Copyright 2012 Mohammad Jafarnejad

ABSTRACT

The lymphatic system plays an important role in fluid and protein balance within the interstitial spaces. Its dysfunction could result in a number of debilitating diseases, namely lymphedema. Lymphatic vessels utilize both intrinsic and extrinsic mechanisms to pump lymph. Intrinsic pumping involves the active contraction of vessels, a phenomenon that is regulated in part by nitric oxide (NO) produced by lymphatic endothelial cells (LECs). NO production by arterial endothelial cells has been shown to be sensitive to both shear stress and stretch. Therefore, because of the unique mechanical environment of the LECs, we hypothesize that mechanical forces play an important role in regulation of the lymphatic pumping. Parallel-plate flow chambers and indenter-based cyclic stretch devices were constructed and used to apply mechanical loads to LECs. In addition, high-throughput micro-scale channels were developed and tested for shear experiments to address the need to increase the productivity and high-resolution imaging. Twenty-four hours treatment of LECs with different shear stress conditions showed a shear-dependent elevation in NO production. Moreover, 2.5 folds increase in cumulative NO was observed for stretched cells compared to the unstretched cells over six hours period. In conclusion, the upregulation observed in NO production under mechanical stimuli suggest new regulatory mechanisms that can be pharmaceutically targeted. These results provide an unprecedented insight into lymphatic pumping mechanism.

ACKNOWLEDGEMENTS

I would like to thank my advisor, Dr. James E. Moore, who always believed in my work and supported my new ideas. I also want to thank my committee members, Dr. Roland R. Kaunas and Dr. David C. Zawieja for their support, guidance, and critical insight throughout this research project.

Special thanks go to my wife, Samira Jamalian, for always believing in me and supporting me even when I did not. She has been the best wife, coworker, and lab-mate for me. In addition, I want to thank my family and friends in my home country who encouraged me to pursue my dreams.

Last but not least, I would like to thank my friends and colleagues who helped me on this work and made Texas A&M University a place full of unforgettable memories for me. In no particular order, John Wilson, Dr. Will Richardson, Dr. Elaheh Rahbar, Chrisine Otieno, Dr. Walter Cromer, Scott Zawieja, Dr. Hsu Su Hsu, Abhishek Tondon, Dr. Peter Walsh, and Dr. Danika Heyman.

Finally, I want to thank Cayman Chemicals for kindly providing a figure from their assay booklet. In addition, I would like to thank Dr. Elaheh Rahbar for generously providing a figure included in this thesis.

NOMENCLATURE

Ca ²⁺	Calcium ion
CO ₂	Carbon dioxide
DAF-FM	4-amino-5-methylamino- 2',7'-difluorescein
DAN	2,3-diaminonaphthalene
DAQ	Data acquisition
DMEM	Dulbecco's modified eagle medium
DMSO	Dimethyl sulfoxide
EDTA	Ethylenediaminetetraacetic acid
EGM-2	Endothelial growth medium-2
eNOS	Endothelial nitric oxide synthase
FBS	Fetal bovine serum
HDLEC	Human dermal lymphatic endothelial cell
HEPES	4-(2-hydroxyethyl)-1-piperazineethanesulfonic acid
LEC	Lymphatic endothelial cell
MCF	Material characterization facility
MV2	Endothelial growth medium MV2
NaOH	Sodium hydroxide
NO	Nitric oxide
NO ₂ ⁻	Nitrite
NO ₃ ⁻	Nitrate

PBS	Phosphate buffer saline
PDMS	Polydimethylsiloxane
RLEC	Rat lymphatic endothelial cell
TFS	(Tridecafluoro-1,1,2,2-tetrahydrooctyl)-1-Trichlorosilane
TNS	Trypsin neutralizing solution
UV	Ultra violet

TABLE OF CONTENTS

	Page
ABSTRACT	ii
ACKNOWLEDGEMENTS.....	iii
NOMENCLATURE	iv
TABLE OF CONTENTS	vi
LIST OF FIGURES.....	vii
1. INTRODUCTION	1
2. METHODS.....	6
2.1. Cell Culture	6
2.2. Fluid Shear Stress Chamber	7
2.3. Stretch Device	8
2.4. Microfluidics Devices	9
2.5. NO Measurement Assay.....	11
2.6. Calcium Imaging	12
2.7. Immunostaining in Micro-Channels	13
3. RESULTS	14
3.1. Shear Dependent NO Production	14
3.2. Stretch-Induced NO Production.....	17
3.3. Shear-Induced Calcium Measurement	20
4. DISCUSSION	25
5. CONCLUSIONS	28
6. REFERENCES	29

LIST OF FIGURES

	Page
Figure 1	Illustration of lymphatic vasculature 2
Figure 2	Schematic diagram of the parallel plate flow loop 7
Figure 3	A schematic of the stretching device is illustrated here..... 9
Figure 4	The two-step reactions of the fluorometric assay is shown here..... 12
Figure 5	The calibration curve plotted for the fluorometric assay done for the shear experiments 14
Figure 6	The NO accumulation plotted versus shear stress..... 15
Figure 7	Phase-contrast images of the cells before and after shear stress treatment..... 16
Figure 8	Calibration curves for the stretch experiments are shown here 17
Figure 9	Accumulated nitrate and nitrite has been plotted for stretch experiments 18
Figure 10	Phase-contrast image of HDLECs has shown before (A) and after (B) 6 hrs of stretch treatment..... 19
Figure 11	The phase-contrast image of the RLECs cultured in the 800 um wide gelatin-coated rectangular channels are shown here.....20
Figure 12	The immunostaining images of the HDLECs in the 800 um channels are shown here.....22
Figure 13	The mean intensity of the fluo-4 representing cytosolic calcium concentration ($[Ca^{2+}]$) in response to shear is plotted here23

1. INTRODUCTION

The lymphatic system is the main regulator of the fluid balance in the tissues and is critical for homeostasis (figure 1). Although the lymphatic system is involved in the maintenance of health and progress of numerous diseases, little is known about the mechanism by which it works and how the various parts function [1-5]. Lymphedema is the most common disease associated with lymphatic system in developed countries. Thirty percent of the 3 million women who survived breast cancer after node dissection or radiotherapy in the United States, have developed lymphedema (i.e., swelling of the areas around the removed node) [6]. Also, this system is the main pathway for the absorption of lipids from the small intestine [7]. In addition, lymph nodes are the home to lymphocytes that play a vital role in the immune response [8]. As lymphatic vessels collect the major part of the interstitial fluid, most of the cancerous tumors metastasize through this system [9]. Recent advances in imaging and measurement techniques have opened unprecedented opportunities for research on the lymphatic system.

Lymphatic system is a one-way drainage path that collects fluid and proteins from the interstitial space and pump it back to venous return located in the shoulder. Thus, there are valves throughout the lymphatic vessels to ensure an efficient unidirectional flow [3]. There are two types of valves in the lymphatic

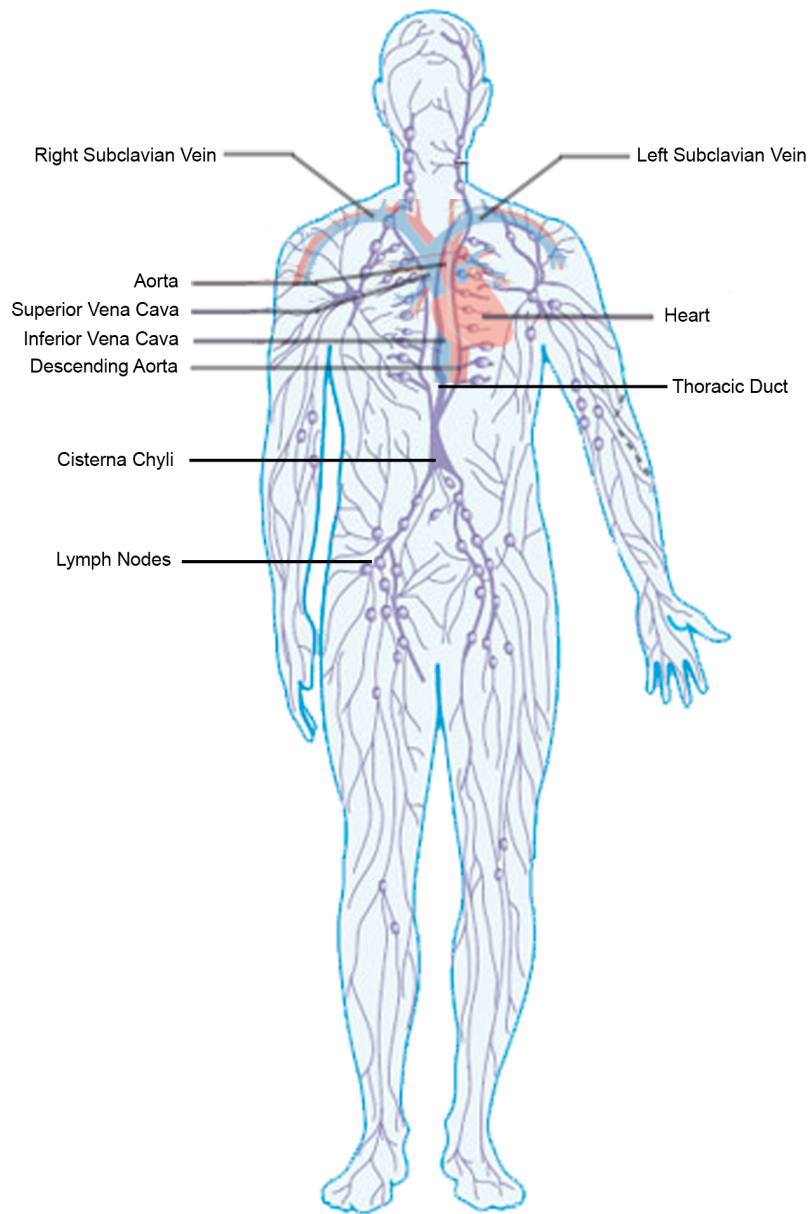


Figure 1. Illustration of lymphatic vasculature. Generously provided by Dr. Elaheh Rahbar.

network: Primary valves that are made of overlapped endothelial cells in the wall of the lymphatic capillaries, and secondary valves that are bi-leaflet valves

present in the pre- and post-nodal collecting lymphatic vessels [4, 10, 11]. Contraction of the lymphatic vessels combined with the ubiquitous valves in the network, results in the one-way flow from interstitial space to the venous return. There are two mechanisms of pumping in the lymphatic system, extrinsic, and intrinsic. Extrinsic pumping is the result of the forces from surrounding of the lymphatic vessel, like arterial pulses, and muscle movements. In contrast, intrinsic pumping is caused by the active contraction of the lymphatic muscle cells wrapped around the collecting lymphatic vessels [3, 4]. This active contraction can generate a unique mechanical environment for endothelial cells.

Numerous studies have addressed the regulatory mechanisms by which arteries and veins respond to mechanical stimuli, but no specific work has been done on the lymphatic endothelial cells [12-16]. The mechanical environment of LECs is very different than other parts of the body, where they experience average shear stresses of less than 1 dyn/cm^2 with the maximum shear as high as 20 dyn/cm^2 [17]. Also the diameter change in lymphatic vessels during a contraction is up to 50%, which makes it unique and completely different than blood circulatory system [17].

Nitric oxide (NO) is a vasodilator in arterial system that is regulated by both wall circumferential stretch and flow shear stress. eNOS is the main catalyzer of the conversion of L-arginin to L-citrulin with NO as the by-product of this reaction. eNOS activation is a Ca^{2+} -calmodulin mediated process. Many studies have measured NO and Ca^{2+} release from vascular endothelial cells

caused by mechanical forces [16, 18-20]. Measurement of NO and Ca^{2+} under mechanical stimuli can reveal if the same process exists for the lymphatic endothelial cells.

Measurement of NO has been always a challenge and different methods have been developed to address this need. Electrochemical electrodes have been used to measure NO both *in situ* and *in vitro* with very high temporal resolution [19, 21, 22]. Bohlen et al. used a custom made electrode to measure NO in mesenteric lymphatic vessels *in situ*. Although *in situ* experiments better show what happens *in vivo*, there is no control on the flow and stretch [21, 22]. Andrews et al. have used a commercial electrode to measure NO from arterial endothelial cells under controlled shear stress, showing an increase in NO production under shear stress [19, 23]. Colorimetric (Griess reaction) and fluorometric assays are other methods for measuring NO_2^- and NO_3^- that are the direct products of NO oxidation in the solution. These are the most reliable methods to measure NO, nonetheless they lack the temporal and spatial resolution, and only accumulation of the nitrate and nitrite can be measured during long periods of stimulation [16, 18, 23]. Intracellular NO-sensitive fluorescent dyes like DAF-FM can be used to investigate the spatial distribution of NO production, but the sensitivity of the dye is low [20]. As mentioned earlier, NO pathway is calcium dependent, so measuring calcium under mechanical stimuli can lead to better understanding of the force induced NO production. Many reliable dyes such as fura-2, and fluo-4 have been developed to measure

intracellular Ca^{2+} . Nauli et al. measured both NO and Ca^{2+} using DAF-FM and fura-2 under shear stress, and showed a rapid increase in both signals peaked at 20 seconds [20]. Interestingly, no direct work has been conducted on the stretch-induced NO and Ca^{2+} change in endothelial cells in vitro.

The focus of this research is to measure NO from LECs under variety of mechanical forces. Aim 1 of this project is to measure NO from LECs under different shear stress magnitudes. The effect of uniaxial cyclic stretch will be studied in aim 2, and finally in aim 3 we will propose a high-throughput micro-scale channel platform for fluorescence-based measurements, specifically the intracellular Ca^{2+} release. To accomplish these goals we need to control the strains and stresses on the cells, which is not possible in *in-vivo*, and *ex-vivo* studies. We have utilized an *in-vitro* approach for this purpose.

2. METHODS

2.1. Cell Culture

Two different cell lines have been used for these studies. A commercial cell line of juvenile human dermal lymphatic endothelial cell (HDLEC) purchased from PromoCell GmbH, and rat mesenteric lymphatic endothelial cells (RLEC) provided generously by Prof. Zawieja in Texas A&M. HDLEC cells have been cultured in micro-vascular endothelial growth medium 2 (MV2) purchased from PromoCell. Endothelial growth medium 2 (EGM2) from Lonza was used for RLECs. The media of the flasks were changed twice a week. To passage cells, cells were first treated with 0.05% trypsin/EDTA, Lonza, followed by 4 minutes 37C incubation. Trypsin neutralizing solution (TNS), Lonza, has been used to deactivate trypsin. The cell solution was centrifuged down at 1000rpm for 5 minutes. After removing the supernatants, pellet was re-suspended in media ready for seeding. To freeze the cells, the pellet was broken using 10% DMSO, and 90% fetal bovine serum (FBS) and transferred to cryogenic tubes. The vials were moved to -80C refrigerator, and then to liquid nitrogen after a day. HDLECs with passages less than 7 and RLECs with passages less than 15 were used for all the experiments.

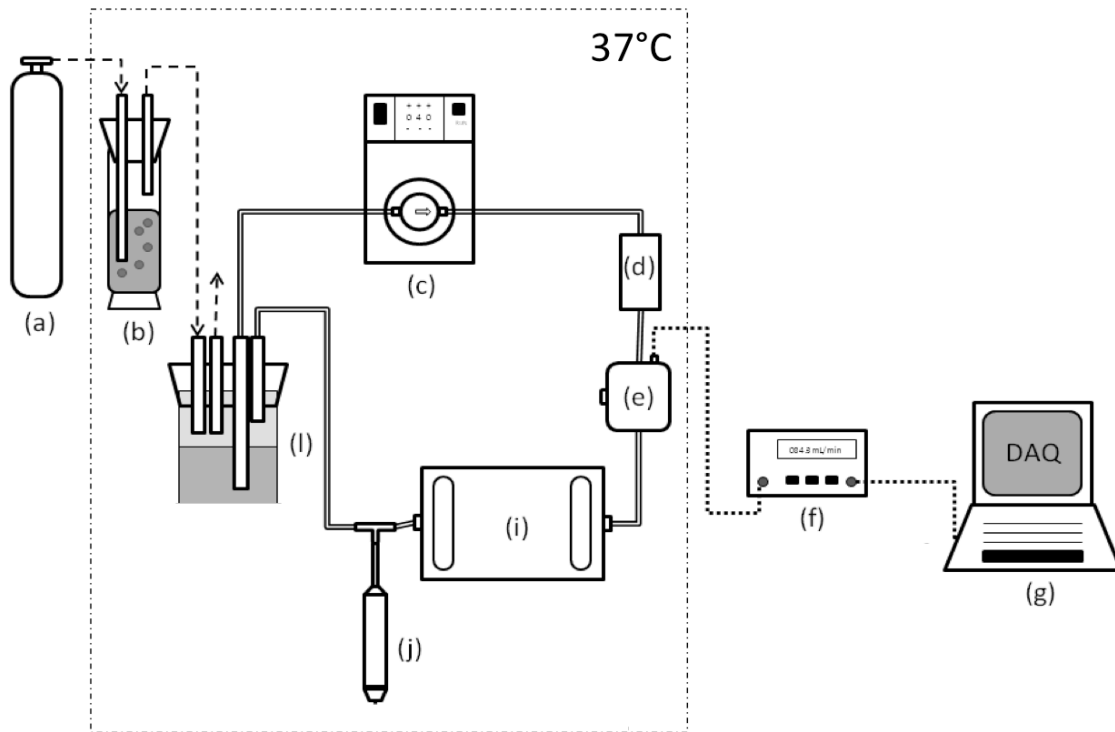


Figure 2. Schematic diagram of the parallel plate flow loop. The entire flow loop is inside a temperature-controlled box. Here are the components of the system: (a) 5%CO₂-95%Air tank, (b) humidifier, (c) gear pump, (d) bubble trap, (e) flowmeter, (i) parallel plate flow chamber, (j) sampling port, (l) reservoir, (f) data acquisition (DAQ) system, (g) pc running DAQ software.

2.2. Fluid Shear Stress Chamber

There are multiple methods to subject endothelial cells to controlled wall shear stress. Cone-and-plate and parallel plate flow chambers are the most common methods for this purpose. Although cone-and-plate needs less media to create the same shear range as parallel plate, the flow pattern in the latter is closer to the one in cylindrical vessels *in vivo*. Many variations of parallel plate flow chambers have been used to study the effect of shear stress on arterial and

venular endothelial cells [14, 16, 18, 19]. The parallel plate used for this study was comprised of an inlet-outlet layer, a gasket, and a glass slide with cells cultured on, all pressed together using a custom made C-clamp (figure 2). The parallel plate was in line with the pump, flow meter, and the reservoir that was constantly supplied by 5%CO₂-95%Air to keep the media oxygenated and pH regulated (figure 2).

2.3. Stretch Device

An Indenter based stretch device capable of producing 10% uniaxial stretch was used to subject endothelial cells to 1Hz cyclic sinusoidal stretch waveform. This custom made device has chambers with silicon membrane at the bottom (figure 3). The stretch will only be uniform in a 4 cm by 4 cm region in the center of the membrane. This region was coated with 10ugr/ml fibronectin for at least 2 hrs before seeding. About $5 \cdot 10^5$ cells were seeded in that area. Experiments were started in a day after seeding.

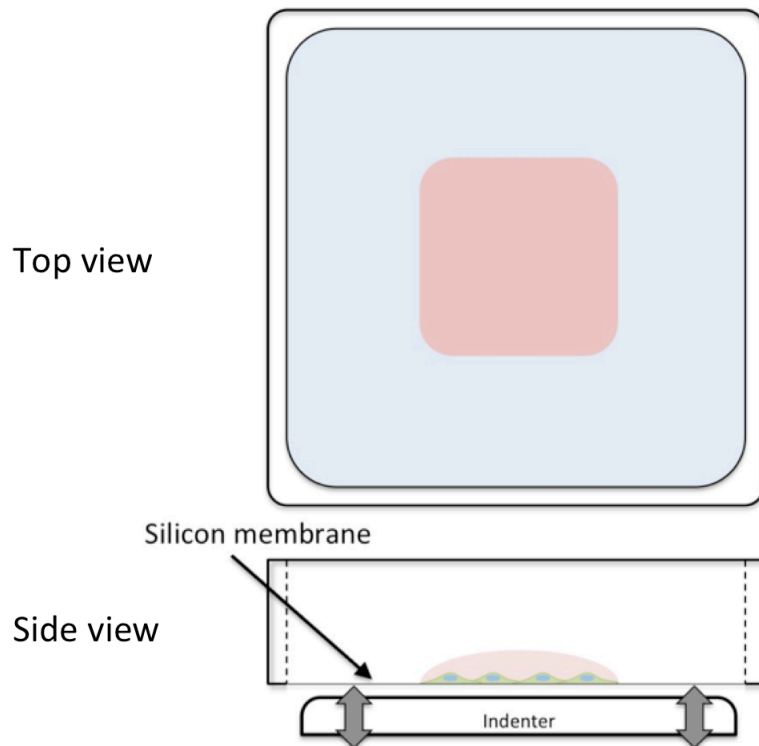


Figure 3. A schematic of the stretching device is illustrated here. The bottom of the chamber is made of a 0.01” thick silicon membrane. The shape of the indenter is so that when it pushes against the membrane, the cultured area will be uniformly stretched uniaxially.

2.4. Microfluidics Devices

Microfluidics devices have been widely used because of their capability in tightly controlling the microenvironment of the cells or tissue, such as mechanical forces, chemical cues, and gradients of those. It also makes the study of the complex and controlled co-culture systems possible. In this study, Micro scale rectangular channels were used to culture lymphatic endothelial cells. Basically, it resembles an integrated parallel plate flow chamber in micro-scale. This method reduces the costs associated with media usage in large-

scale parallel plate chambers, and at the same time it enables the high-throughput shear experiment in channels with different media formulation or pre-conditioning. The idea of shear experiments in micro-channels started with commercially available biochips (Vena8) from Cellix Ltd. Ireland. The disadvantage is that the Vena8 chips are made of impermeable plastic that makes the long-term culture of endothelial cells impossible due to hypoxia and PH changes in the middle of the channels. The problems in long-term culture in commercial products combined with the need for more control in the flow pattern and geometries led us to construct our own custom designed micro-chips.

Standard photolithography was used to fabricate the master molds. Briefly, a 100-120 um film of SU-8 2050, a negative photoresist, purchased from MicroChem was coated on 3 inches silicone wafers purchased from Silicone Quest. The wafers were soft backed for more than 2 hrs at 65C followed by a 95C backing for 45 minutes. All these should be done on a hotplate rather than an oven; otherwise, solvent removal from the surface causes the surface to wrinkle. The dark-field masks were designed in Solidwroks and printed by CAD/Art with 25400 dpi, capable of printing patterns with 10 um features. The soft baked wafers were then exposed with 250 J/cm² UV light using the mask aligner in material characterization facility (MCF) at Texas A&M. The UV exposed parts of the SU-8 crosslinks and solidifies. A hard baking step was performed with 30 minutes at 65C followed by 45 minutes at 95C to remove all the solvents from the film. The wafers relaxed at room temperature for at least 2

hrs and then developed in SU-8 developer from MicroChem. The developer dissolves the uncrosslinked SU-8 leaving the exposed pattern on the wafers. The height of the pattern can be measured by profilometer to confirm the channel heights. The wafers were coated by (Tridecafluoro-1,1,2,2-tetrahydrooctyl)-1-Trichlorosilane (TFS) to facilitate the PDMS removal. The PDMS channels were then replicated from molds using standard soft-lithography.

Sylgard 184 was mixed in 1:10 ratio of curing agent to base. The mixture was degassed in desiccator and poured on the wafers attached to the bottom of the petri dishes. The PDMS parts were then cured in 80C oven. Inlet hole punched using 2mm dermal punches and the surfaces were cleaned by non-stick scotch tape. Afterwards, the PDMS parts were wet autoclaved in DI water followed by a dry autoclave and then 24 hrs of drying in 80C oven. The PDMS fluidic layers were then bond to No.1 cover glasses using plasma treatment. The cover-glass bottom chambers enable us to perform high resolution imaging, which is not possible by glass slide bottom parallel plate chambers.

2.5. NO Measurement Assay

“Nitrate/nitrite fluorometric assay kit” purchased from Cayman Chemicals was used to measure the accumulated nitrate and nitrite in the media samples. First, the nitrate content of the samples was converted to nitrite using nitrate reductase enzyme. In the second step, the addition of DAN resulted in a fluorescent product, and the fluorescence was enhanced using NaOH (figure 4).

20 uL media samples were needed to perform the assay. Calibration curves produced in the presence of each type of media separately.

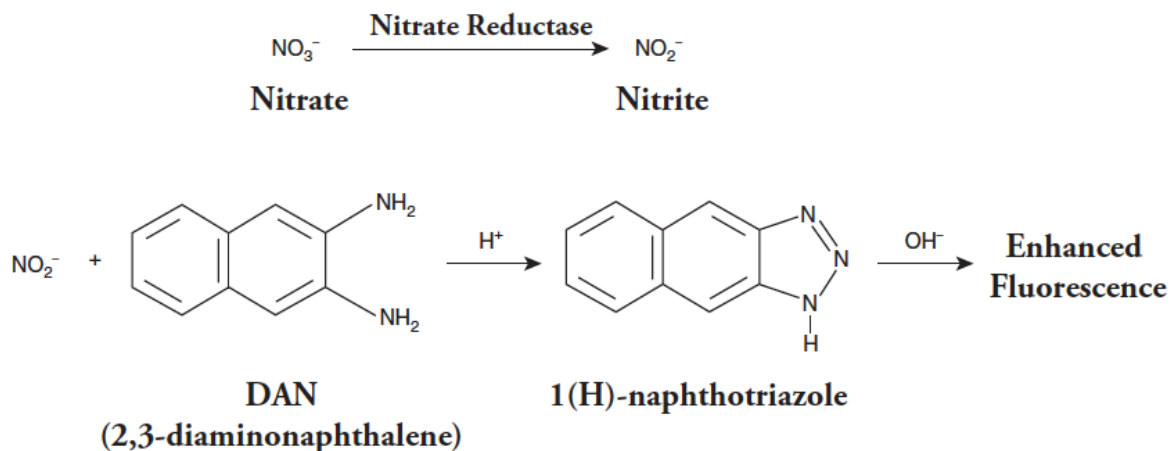


Figure 4. The two-step reactions of the fluorometric assay is shown here. First, nitrate (NO_3^-) converted to nitrite (NO_2^-) using nitrate reductase enzyme (top reaction). Then the reaction of DAN with the total nitrite resulted in a fluorescence molecule (1(H)-naphthotriazole), followed by the addition of NaOH to enhance the fluorescence signal. Adapted from nitrate/nitrite fluorometric assay booklet, Cayman Chemicals, Michigan.

2.6. Calcium Imaging

Fluo-4 AM purchased from Molecular probes, Invitrogen was used to measure cytosolic calcium in response to shear stress. 50 ugr of the Fluo-4 AM was diluted into 20% w/v pluronic/DMSO solution to a final concentration of 5 mM. Then the stock solution was diluted in the DMEM F-12 media to 10 uM. This media is a comparatively CO_2 independent with 15 mM HEPES, and does not contain albumin to avoid dye removal. Cells were loaded for 1 hr at 37C

incubator, followed by a 30 minutes de-esterification in F-12 media. Finally, the cells were imaged using an open pinhole confocal microscope with 488nm excitation laser. The fluorescence intensity of the dye is proportional to the cytosolic calcium.

2.7. Immunostaining in Micro-Channels

Cells were fixed at room temperature in 2% paraformaldehyde in phosphate buffer saline (PBS) for 30 minutes. Then, cells were washed with PBS continuously for 5 minutes, and blocked with 5% goat serum in PBS for 2 hrs. 1:200 dilution of primary antibody was used over night at 4C. On the next day, cells were washed with the wash buffer (PBS with 0.05% Tween-20) followed by the treatment of 1:200 diluted secondary antibody for 2 hrs, and then wash again. At the end, the channel was filled with anti-fade reagent.

3. RESULTS

3.1. Shear Dependent NO Production

We measured NO produced by HDLECs under shear stress and showed an increase in cumulative NO over 24 hrs of shear treatment. Parallel plate flow chambers described in the methods section used to treat cells with shear stresses ranging from 1-12 dyn/cm² to cover the physiologic shear stress range

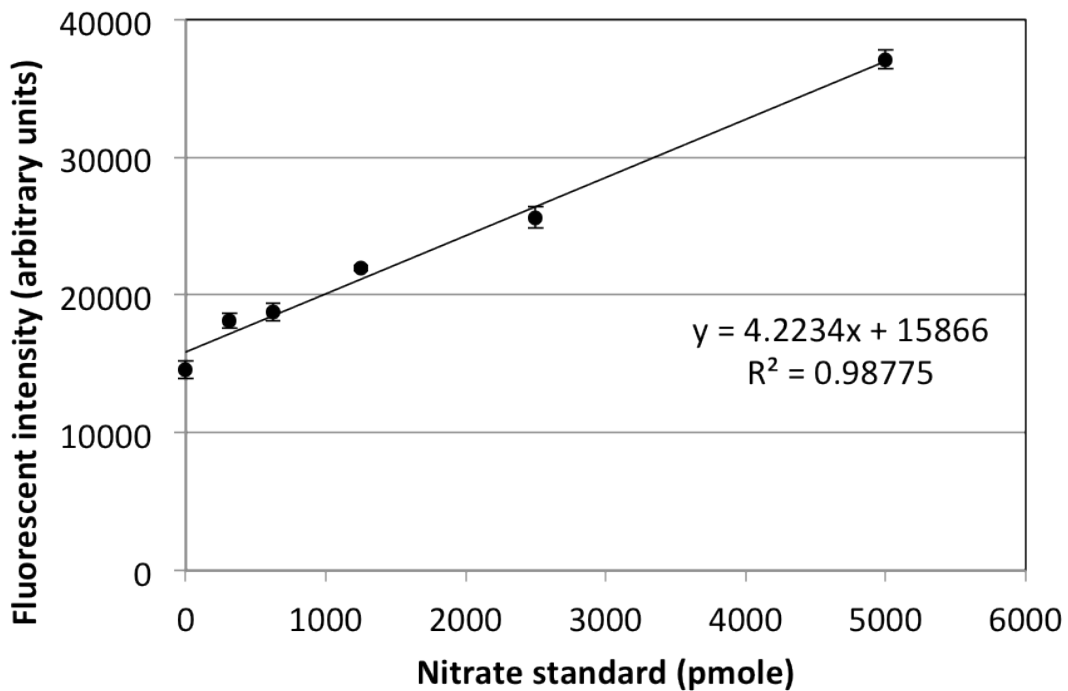


Figure 5. The calibration curve plotted for the fluorometric assay done for the shear experiments. The values are mean \pm standard deviation, with $n=3$. The equation is the linear fit to the data points used to convert the intensity readings to NO moles.

in the lymphatic system. Media samples were taken right at the beginning of the experiments, and after 24 hrs of shear stress. Fluorometric assay was used to measure the accumulated nitrate and nitrite that are the final products of NO oxidation. The difference between the two samples in each experiment was reported as the cumulative NO produced over 24 hrs (figure 6). The measures have been normalized over the total number of cells in each experiment. Figure 5 shows the calibration curve for the assay that was performed for this set of

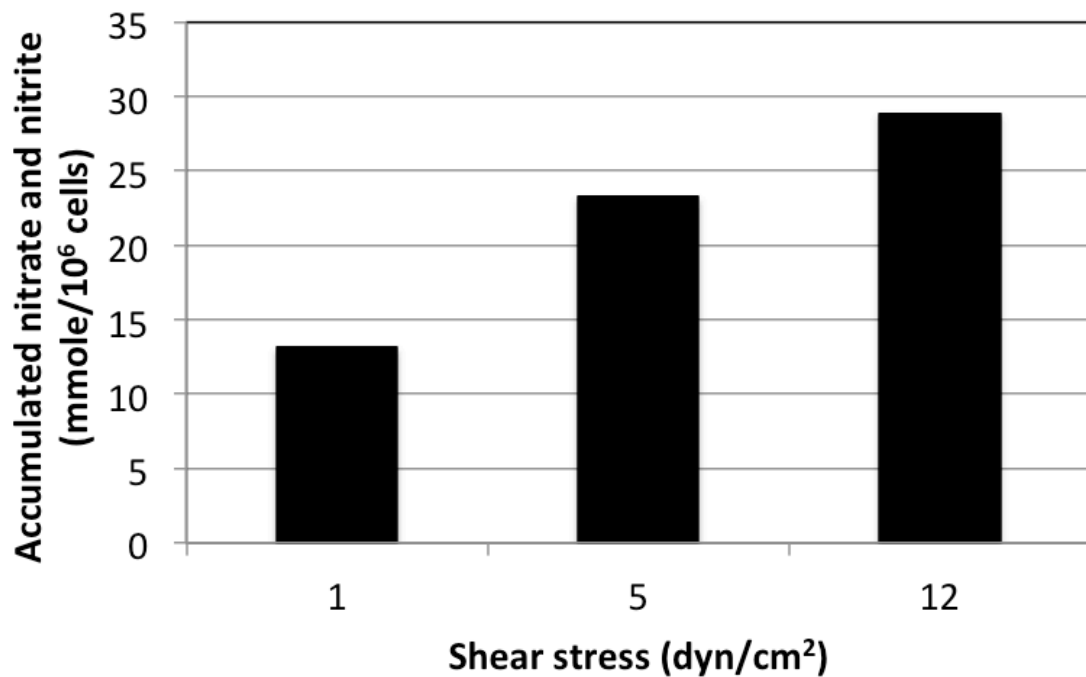


Figure 6. The NO accumulation plotted versus shear stress. The values are the average of two experiments for 1 dyn/cm², and one for each of 5 and 12 dyn/cm². Data has been normalized by the approximate number of the cells in each experiment obtained from phase-contrast images.

experiments. The linearity of the curve even in the low concentrations implies a reliable assay. HDLECs exhibited sensitivity to shear stress by producing more NO as the shear increased.

As expected, HDLECs oriented in and elongated to the direction of the flow when shear stress increased. Figure 7 represents images of the cells before and after shear stress treatment. Only cells under 12 dyn/cm^2 showed significant elongation and reorientation. The endothelial cell monolayer checked after the experiment to ensure it remained intact for all the experiments.

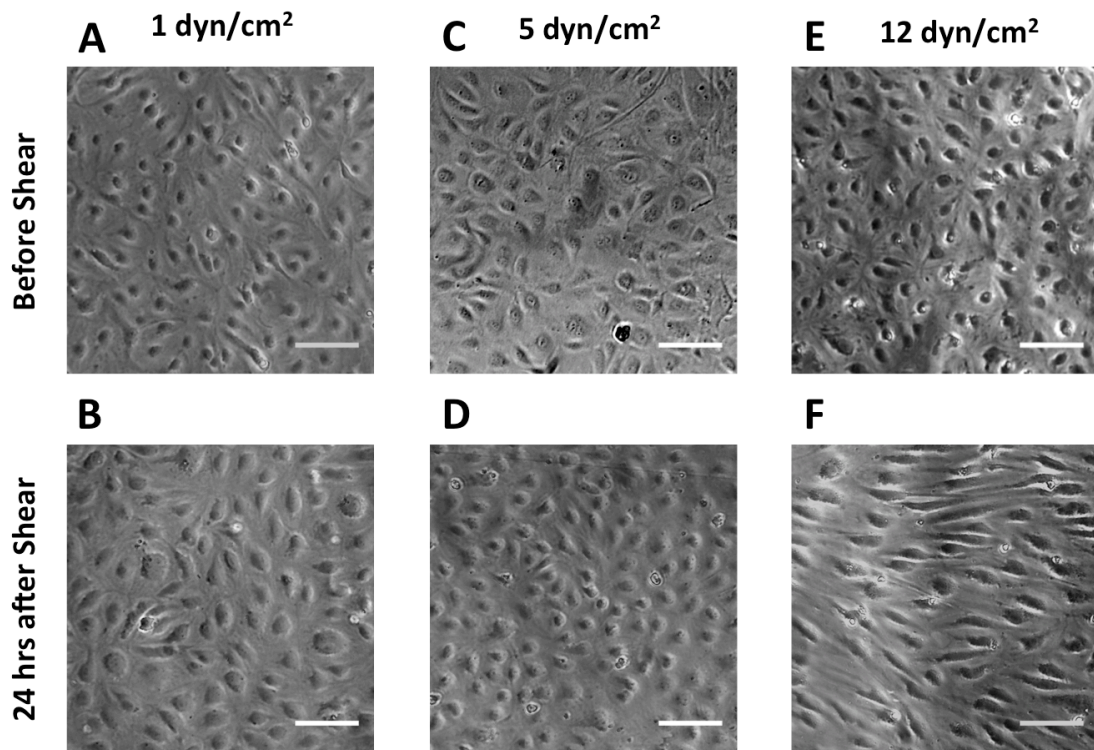


Figure 7. Phase-contrast images of the cells before and after shear stress treatment. The top images show the cells before the shear starts, and the ones at the bottom show the cells after 24 hrs of shear treatment. The flow direction is from left to right in all the images, and scale bars are 100 μm .

3.2. Stretch-Induced NO Production

2.5-fold increase in accumulated nitrate and nitrite was observed from HDLECs and RLECs under 1 Hz sinusoidal cyclic stretch after 6 hrs. Calibration curve was produced for each media type to increase the accuracy in analyzing the data (figure 8). The total nitrate and nitrite per centimeter square of culture was measured and reported for the control and stretched cases. Both cell types

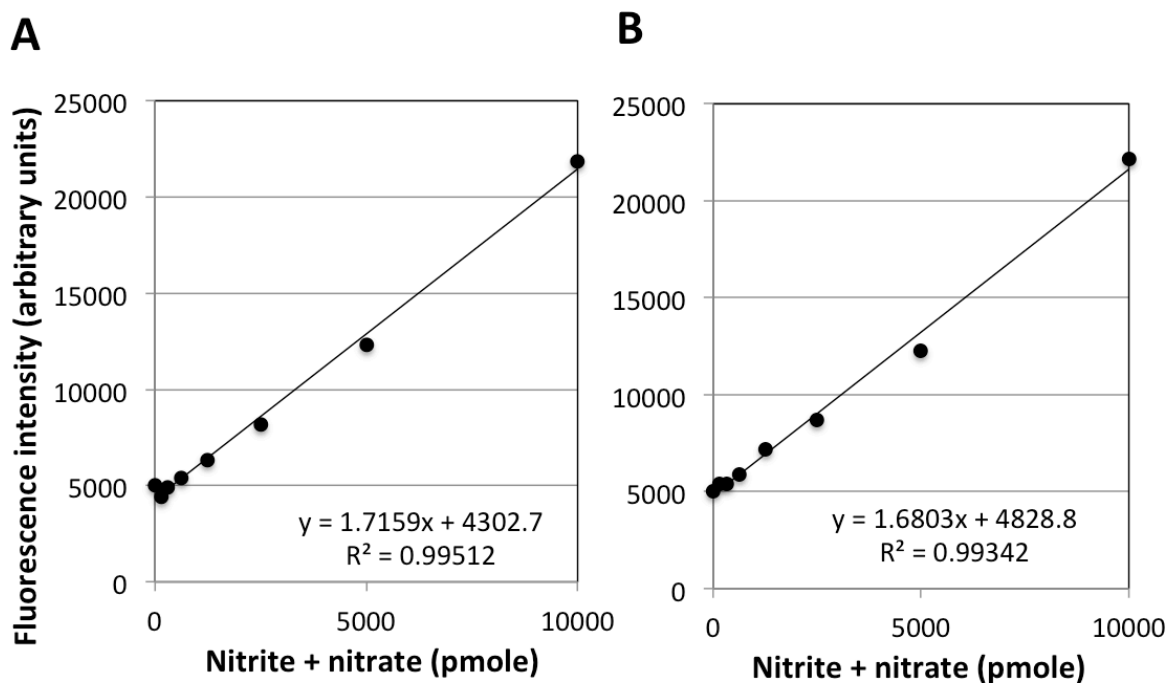


Figure 8. Calibration curves for the stretch experiments are shown here. The panel A is the calibration plot in the presence of HDLEC media, and the panel B is the calibration curve in the presence of RLEC media. The vertical axes show fluorescence intensity, and the horizontal axes represent concentrations of nitrate standard solutions. The equations are the linear fits to the data points.

showed an upregulation of about 2.5 fold in NO production under cyclic stretch (figure 9). Furthermore, the NO production level was almost double in HDLECs

compared to RLECs. All these similarities and differences are present while these cell types are from two different species, HDLECs from human and RLECs from rat, and also they are from two different locations in the body, HDLECs from foreskin and RLECs from mesentery. The results showed statistical significance in student's t-test with $p < 0.01$. We demonstrated that both lymphatic endothelial cell lines show similar increase in NO production over a 6 hrs cyclic stretch.

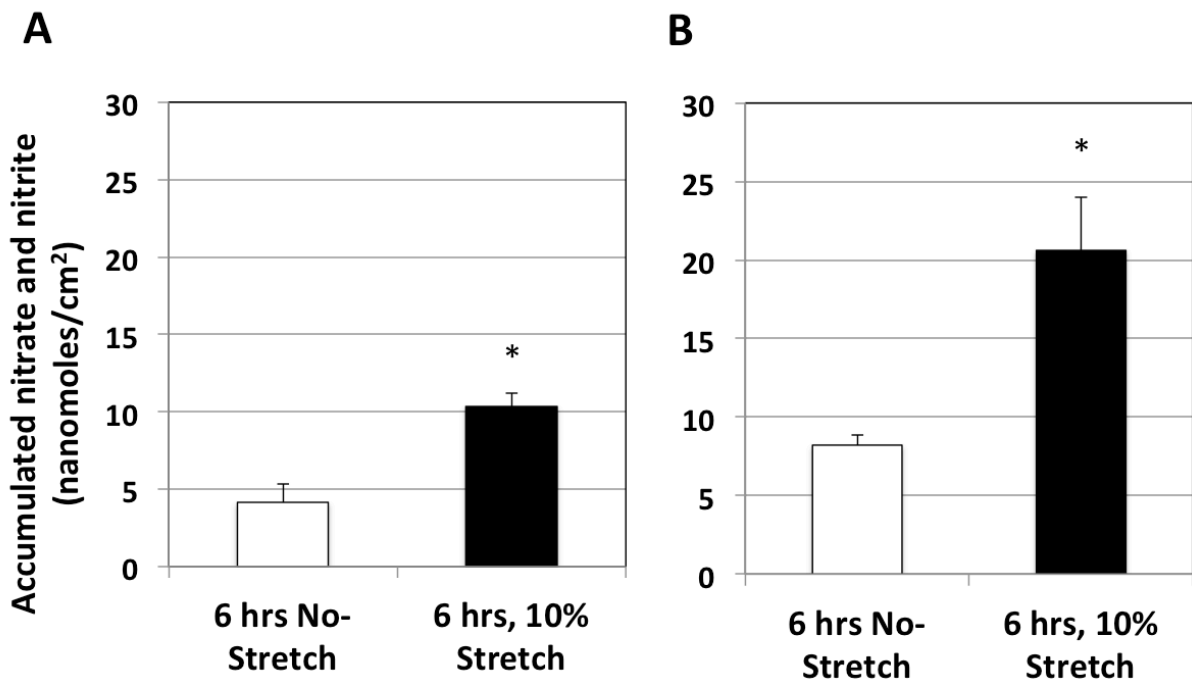


Figure 9. Accumulated nitrate and nitrite has been plotted for stretch experiments. Panel A shows the NO produced in LECs with and without 6 hrs of 10%, 1 Hz, uniaxial stretch for the RLECs, and the panel B shows the corresponding results for the HDLECs. Data are presented as mean \pm standard deviation, with $n=3$, and $p < 0.01$.

As expected, both cell lines showed alignment perpendicular to the direction of stretch. Figure 10 shows a typical experiment with HDLECs before and after the 6 hrs 1 Hz cyclic stretch. Polarization and alignment of endothelial cells in the vertical direction is demonstrated in figure 10-B, which is perpendicular to the horizontal uniaxial stretch direction. The same alignment was observed in the RLECs after 6 hrs of stretch. The phase-contrast images of the cells before and after cyclic uniaxial stretch showed elongation of the lymphatic endothelial cells perpendicular to the direction of stretch.

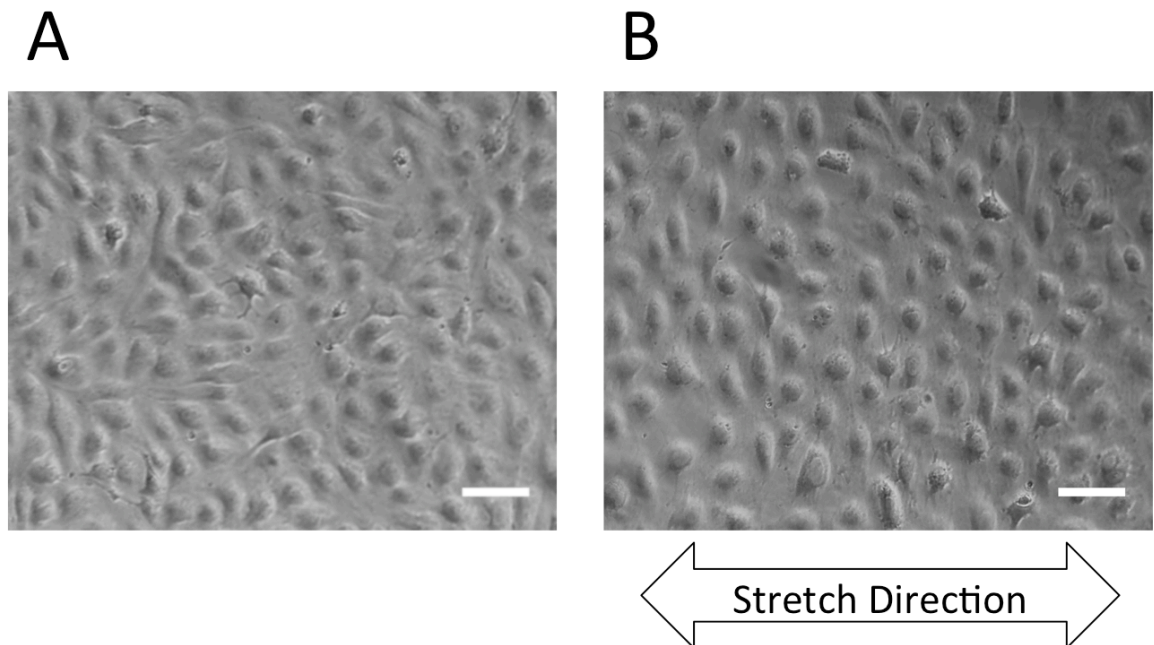


Figure 10. Phase-contrast image of HDLECs has shown before (A) and after (B) 6 hrs of stretch treatment. The uniaxial stretch is in horizontal direction (as shown by the arrow), and scale bars are 100 μm .

3.3. Shear-Induced Calcium Measurement

A high-throughput miniaturized parallel plate platform was developed to study the effect of acute and chronic shear stress on lymphatic endothelial cells. As explained extensively in the methods section, channels with 120 μm heights

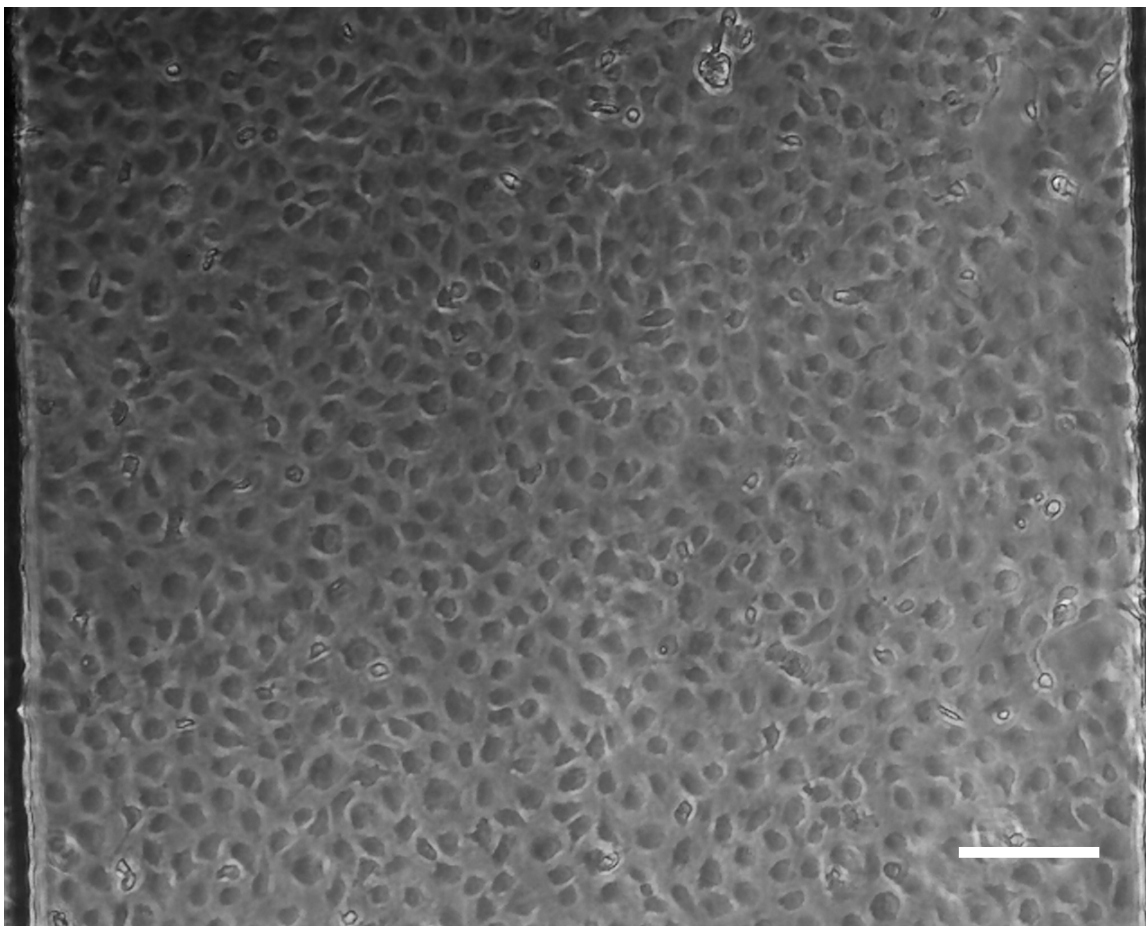


Figure 11. The phase-contrast image of the RLECs cultured in the 800 μm wide gelatin-coated rectangular channels are shown here. Cells have been in culture for 12 days. Scale bare is 100 μm .

were manufactured using soft-lithography, and a protocol was optimized for long-term culture of lymphatic endothelial cells. Figure 11 is an image of 800 μm wide channel with RLECs cultured inside. Seeding density of 5×10^6 cells/ml was shown to be the optimum to seed both cell types in the micro-channels. Both cell types were cultured on variety of substrate proteins such as fibronectin, collagen-I, and gelatin. HDLECs grew very well on all three types of matrix proteins. On the other hand, RLECs proliferate good on gelatin, fibronectin, and high concentrations of collagen-I, but not in the channels coated with concentrations less than 1 gr/ml. As only very small volume (10 μL) of cell solution is needed for seeding in the channels, many of them can be seeded at the same time and treated with different conditions for the experiments. A programmable syringe pump can be utilized to produce acute shear stresses in any required ranges. A continuous pump is needed for chronic shear treatments, which can be done in parallel for many channels. Briefly, we demonstrated a high-throughput micro-channel setup for chronic and acute shear experiments of lymphatic endothelial cells.

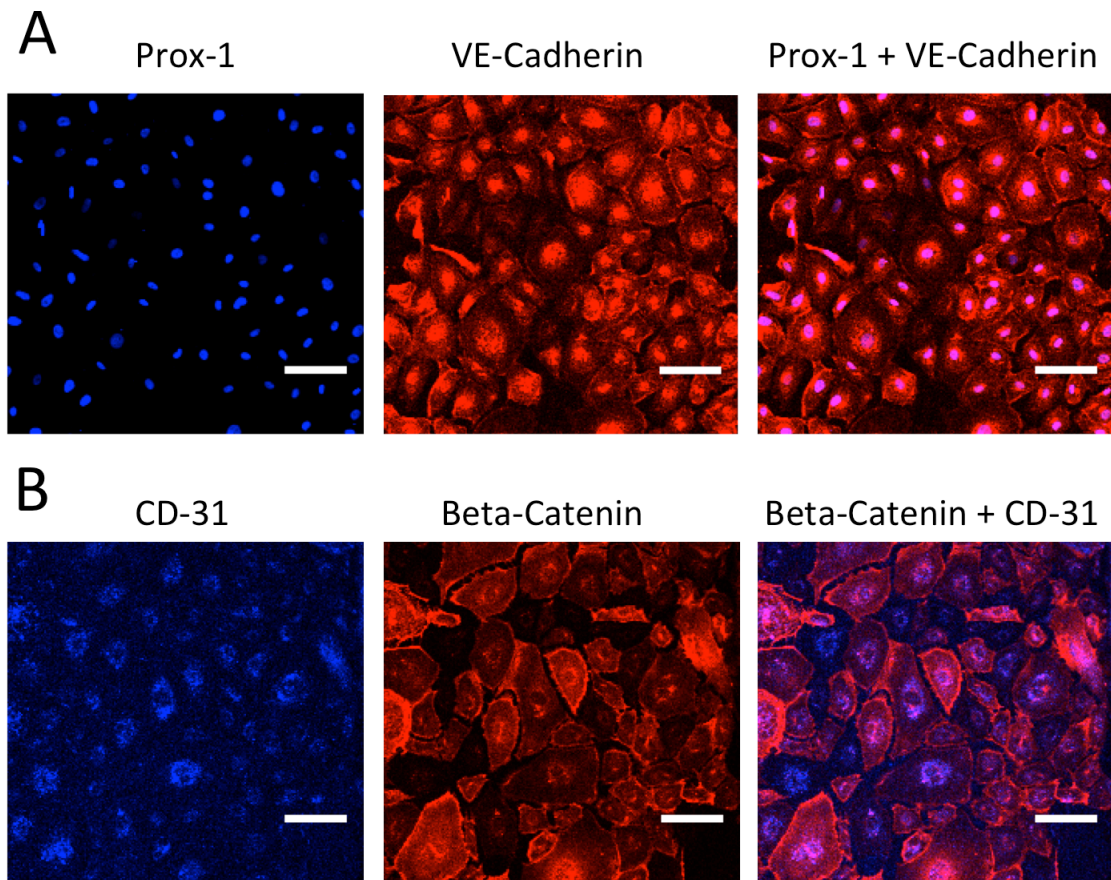


Figure 12. The immunostaining images of the HDLECs in the 800 um channels are shown here. In one channel cells were double stained for Prox-1 and VE-cadherin (A), and in another channel, they were stained for CD-31 and beta-catenin. Scale bar is 100um.

In addition, we have shown that the micro-channels are suitable for immunostaining. HDLECs cultured on fibronectin were stained by the protocol explained before. Figure 12-A shows the results of the double staining for Prox-1, a lymphatic endothelial cell marker, and VE-cadherin, a cell-cell junction protein. CD-31 and Beta-catenin, two other junction proteins were stained in

another channel (figure 12-B). The capability of the high quality immunostaining in these channels broadens the use of them in future applications.

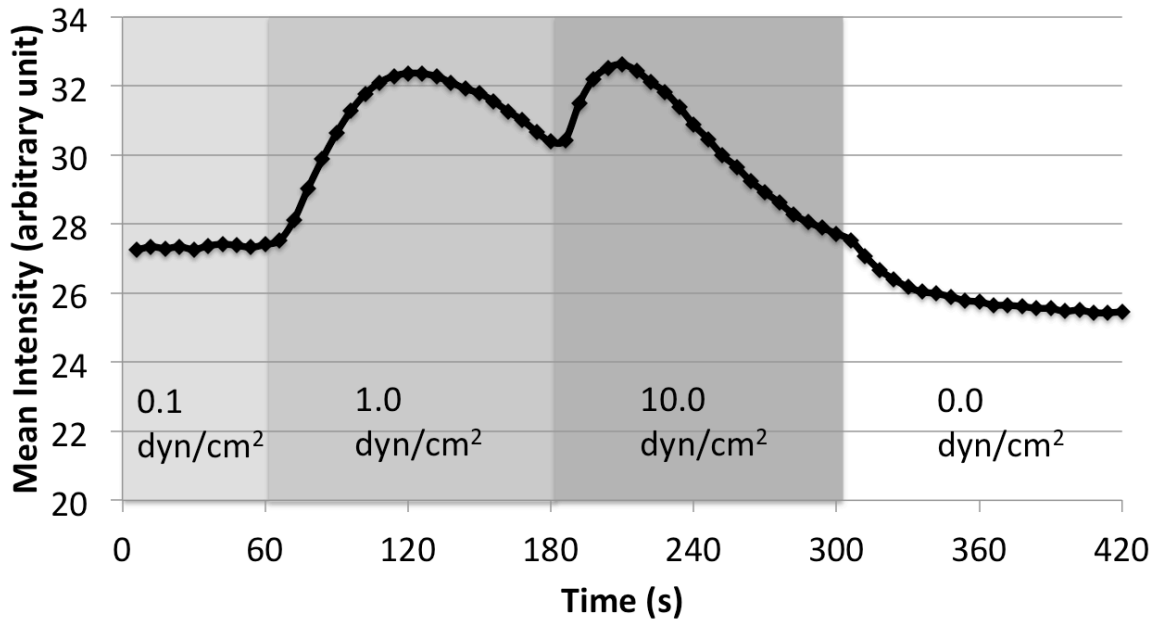


Figure 13. The mean intensity of the fluo-4 representing cytosolic calcium concentration ($[Ca^{2+}]$) in response to shear is plotted here. The HDLECs were cultured to confluent on gelatin matrix in 800 wide channels were used for this experiment. The step increases in shear started after the baseline signal was obtained under 0.1 dyn/cm² shear stress.

Furthermore, live intracellular calcium imaging was conducted on HDLECs cultured in the channels under shear stress. Calcium dynamics in endothelial cells is important because it regulates many pathways, one of which is NO production pathway. Here, we showed that a step increase in shear stress causes an instantaneous release of calcium from intracellular reservoirs measured by Fluo-4 intracellular calcium dye. Figure 3 shows the changes in

mean intensity of the image over time in response to changes in shear stress noted in the images.

4. DISCUSSION

Nitric oxide has been studied extensively in arterial system as the most important vasoactive chemical; however its role in lymphatic system is still under investigation. A recent study has shown an increase in lymphatic flow rate in an edematous rat model [unpublished data]. In addition, Bohlen et al. has measured NO *in situ* from mesenteric lymphatic vessels using custom-made electrochemical sensors [21, 22]. They have shown increase in diameter, decrease in vessel tone, and decrease in contraction frequency when flow was increased and higher NO concentration was measured. In this study we utilized an *in vitro* approach to investigate if NO response of the lymphatic endothelial cell is shear sensitive. From the many available methods of NO measurement, fluorometric assay was the only method that had reliable responses with the least possible noise level in our setup. Although the NO electrodes have the ideal temporal resolution, they showed a high sensitivity to temperature changes that made it unpractical to be decoupled from flow. Also, DAF-FM with detailed spatial resolution proved to have very low NO sensitivity to be used for measurements in lymphatic endothelial cells. The limitation of the fluorometric assay is the lack of any spatial or temporal resolution. More experiments need to be done to make sure the results have been repeatable and the differences are significant for shear experiments.

Macro-scale parallel plate flow chambers have been traditionally used to study the effect of flow on endothelial cells [14, 16, 19, 20]. To amplify the signal from accumulated nitrate and nitrite, one needs to minimize the flow loop volume. In this case a gear pump was chosen over roller pump to remove the damper, which could have increased the dead volume of the circuit. Also as the mean flow rate in lymphatic system is less than 1 dyn/cm^2 , a case with shear less than 1 dyn/cm^2 can better represent the behavior of the lymphatic endothelial cells in the lower shear ranges.

Presence of valve and sinus bulb in the lymphatic vessels leads to the complicated wall motion during contraction. Our results on the effect of stretch on lymphatic endothelial cells from two different locations in the body (mesentery vs. skin), and from two different species (human vs. rat) showed the same regulatory behavior. Not much work has been done on the effect of stretch on NO production even in arterial endothelial cells. The current study has been done under 1 Hz sinusoidal stretch pattern. To better understand the effect of physiologic stretch waveform on the lymphatic endothelial cells, a stretching device capable of generating controlled stretch waveforms is necessary.

Higher throughput systems are required to increase the productivity and reduce the costs. We developed and tested micro-channels to study the effect of acute and chronic shear stress on lymphatic endothelial cells. This platform let us run many parallel shear experiments under different conditions. In addition to the capabilities of the conventional parallel plate flow chambers, the cover glass

bottom micro-channels enable us to take high magnification images of the cells, while they use less cells and media. The results of the calcium measurements done here are comparative to studies done on aortic embryonic endothelial cells by Nauli et al. [20]. More repetition of this experiment is needed to see how reproducible the signal is.

5. CONCLUSIONS

In this study, we investigated the effect of mechanical stimuli like shear stress and stretch on NO production of the lymphatic endothelial cells. HDLECs exhibited an increase in NO production by increase in shear stress, a behavior that has been shown in the arterial endothelial cells before. In stretch experiments, we observed a 2.5 fold increase in NO production after 6 hrs of 10% cyclic stretch. Furthermore, the baseline NO production in the HDLECs was double the amount of RLECs. Also a microfluidic platform was developed to treat the cells with acute and chronic shear stresses, and the culture protocol was finalized. In addition, we demonstrated how the immunostaining, and real-time calcium imaging in response to shear is possible in this new platform. The results of this study can be directly used in computational modeling of the lymphatic system as the input parameters, and also as a baseline for future experiments related to lymphatic mechanics related.

6. REFERENCES

- [1] Radhakrishnan, K., and Rockson, S. G., 2008, "The clinical spectrum of lymphatic disease," *Annals of the New York Academy of Sciences*, 1131(1), pp. 155-184.
- [2] Rockson, S. G., 2010, "Causes and consequences of lymphatic disease," *Annals of the New York Academy of Sciences*, 1207, pp. E2-E6.
- [3] Zawieja, D., 2005, "Lymphatic biology and the microcirculation: past, present and future," *Microcirculation*, 12(1), pp. 141-150.
- [4] Schmid-Schonbein, G. W., 1990, "Microlymphatics and lymph flow," *Physiological Reviews*, 70(4), pp. 987-1028.
- [5] Rockson, S. G., 2008, "Diagnosis and management of lymphatic vascular disease," *Journal of the American College of Cardiology*, 52(10), pp. 799-806.
- [6] Rockson, S. G., and Rivera, K. K., 2008, "Estimating the population burden of lymphedema," *Annals of the New York Academy of Sciences*, 1131(1), pp. 147-154.
- [7] Dixon, J. B., 2010, "Lymphatic lipid transport: sewer or subway?," *Trends in Endocrinology & Metabolism*, 21(8), pp. 480-487.
- [8] Swartz, M. A., Hirose, S., and Hubbell, J. A., 2012, "Engineering approaches to immunotherapy," *Science Translational Medicine*, 4(148), p. 148rv149.
- [9] Shields, J. D., Fleury, M. E., Yong, C., Tomei, A. A., Randolph, G. J., and Swartz, M. A., 2007, "Autologous chemotaxis as a mechanism of tumor cell homing to lymphatics via interstitial flow and autocrine CCR7 signaling," *Cancer Cell*, 11(6), pp. 526-538.
- [10] Mendoza, E., and Schmid-Schonbein, G. W., 2003, "A model for mechanics of primary lymphatic valves," *Journal of Biomechanical Engineering* 125(3), pp. 407-414.
- [11] Schmid-Schonbein, G. W., 2003, "The second valve system in lymphatics," *Lymphatic Research and Biology*, 1(1), pp. 25-31.

- [12] Garanich, J. S., Pahakis, M., and Tarbell, J. M., 2005, "Shear stress inhibits smooth muscle cell migration via nitric oxide-mediated downregulation of matrix metalloproteinase-2 activity," *American Journal of Physiology - Heart and Circulatory Physiology*, 288(5), pp. H2244-H2252.
- [13] Chiu, J.-J., Usami, S., and Chien, S., 2009, "Vascular endothelial responses to altered shear stress: Pathologic implications for atherosclerosis," *Annals of Medicine*, 41(1), pp. 19-28.
- [14] Li, Y.-S. J., Haga, J. H., and Chien, S., 2005, "Molecular basis of the effects of shear stress on vascular endothelial cells," *Journal of Biomechanics*, 38(10), pp. 1949-1971.
- [15] Uematsu, M., Ohara, Y., Navas, J. P., Nishida, K., Murphy, T. J., Alexander, R. W., Nerem, R. M., and Harrison, D. G., 1995, "Regulation of endothelial cell nitric oxide synthase mRNA expression by shear stress," *American Journal of Physiology - Cell Physiology*, 269(6), pp. C1371-C1378.
- [16] Corson, M. A., James, N. L., Latta, S. E., Nerem, R. M., Berk, B. C., and Harrison, D. G., 1996, "Phosphorylation of endothelial nitric oxide synthase in response to fluid shear stress," *Circulation Research*, 79(5), pp. 984-991.
- [17] Dixon, J. B., Greiner, S. T., Gashev, A. A., Cote, G. L., Moore, J. E., and Zawieja, D. C., 2006, "Lymph flow, shear stress, and lymphocyte velocity in rat mesenteric prenodal lymphatics," *Microcirculation*, 13(7), pp. 597-610.
- [18] Kuchan, M. J., and Frangos, J. A., 1994, "Role of calcium and calmodulin in flow-induced nitric oxide production in endothelial cells," *American Journal of Physiology - Cell Physiology*, 266(3), pp. C628-C636.
- [19] Andrews, A. M., Jaron, D., Buerk, D. G., Kirby, P. L., and Barbee, K. A., 2010, "Direct, real-time measurement of shear stress-induced nitric oxide produced from endothelial cells in vitro," *Nitric Oxide*, 23(4), pp. 335-342.
- [20] Nauli, S. M., Kawanabe, Y., Kaminski, J. J., Pearce, W. J., Ingber, D. E., and Zhou, J., 2008, "Endothelial cilia are fluid shear sensors that regulate calcium signaling and nitric oxide production through polycystin-1," *Circulation*, 117(9), pp. 1161-1171.
- [21] Bohlen, H. G., Wang, W., Gashev, A., Gasheva, O., and Zawieja, D., 2009, "Phasic contractions of rat mesenteric lymphatics increase basal and phasic nitric oxide generation in vivo," *American Journal of Physiology - Heart and Circulatory Physiology*, 297(4), pp. H1319-H1328.

[22] Bohlen, H. G., Gasheva, O. Y., and Zawieja, D. C., 2011, "Nitric oxide formation by lymphatic bulb and valves is a major regulatory component of lymphatic pumping," *American Journal of Physiology - Heart and Circulatory Physiology*, 301(5), pp. H1897-H1906.

[23] Lane, W. O., Jantzen, A. E., Carlon, T. A., Jamiolkowski, R. M., Grenet, J. E., Ley, M. M., Haseltine, J. M., Galinat, L. J., Lin, F.-H., Allen, J. D., Truskey, G. A., and Achneck, H. E., 2012, "Parallel-plate flow chamber and continuous flow circuit to evaluate endothelial progenitor cells under laminar flow shear stress," *J Vis Exp*(59), p. e3349.